Enhanced figure of merit of a porous thin film of bismuth antimony telluride

Makoto Kashiwagi,[1,2,a)] Shuzo Hirata,[3] Kentaro Harada,[1,3] Yanqiong Zheng,[1,2]
Koji Miyazaki,[1,2,b)] Masayuki Yahiro,[1,3,4] and Chihaya Adachi[1,3,c)]
[1]*Life BEANS Center Kyushu, BEANS Laboratory, 744 Motooka, Nishi-ku, Fukuoka 819-0395, Japan*
[2]*Department of Mechanical and Control Engineering, Kyushu Institute of Technology, 1-1 Sensui-cho,
Tobata-ku, Kitakyushu 804-8550, Japan*
[3]*Center for Organic Photonics and Electronics Research (OPERA) and Center for Future Chemistry,
Kyushu University, 744 Motooka, Nishi-ku, Fukuoka 819-0395, Japan*
[4]*Institute of Systems, Information Technologies and Nanotechnologies, 203-1 Motooka, Nishi-ku,
Fukuoka 814-0111, Japan*

A porous thin film of $Bi_{0.4}Te_3Sb_{1.6}$ with an enhanced figure of merit of 1.8 at room temperature was fabricated by flash evaporation on an alumina substrate containing hexagonally arranged nanopores with an average diameter of 20 nm, separated by an average distance of 50 nm. The thermal conductivity was significantly reduced compared with standard $Bi_{0.4}Te_3Sb_{1.6}$ films to 0.25 W/(m·K) with no major decrease in either the electrical conductivity (398 S/cm) or the Seebeck coefficient (198 μV/K). The reduction in thermal conductivity was rationalized using a model for the full distribution of the phonon mean free path in the film. © *2011 American Institute of Physics.* [doi:10.1063/1.3543852]

Thermoelectric generators can partially convert low grade waste heat into electricity, making it a key technology to contribute to sustainability through the scavenging of waste heat.[1] Their efficiency is calculated by the thermoelectric figure of merit *ZT*, which is defined as

$$ZT = (\sigma S^2/\lambda)T, \qquad (1)$$

where σ is the electrical conductivity, S is the Seebeck coefficient, T is the temperature, and λ is the thermal conductivity. To date, thermoelectrics have, in general, been too inefficient to be cost effective in most applications. Therefore, many attempts to enhance the figure of merit using nanostructured materials have been made over the past 20 years.[1,2] It has been increasingly recognized that thermal conductivity in nanostructured materials is not an intrinsic parameter as it is for bulk materials.[3,4] In particular, recent studies on Bi_2Te_3–Sb_2Te_3 superlattices,[5] PbTe–PbSe quantum dot superlattices,[6] and Si nanowires[7] have shown that significant reduction of the thermal conductivity is induced by strong phonon scattering. We focused on the low thermal conductivity of nanoporous materials.[8] However, electrical conductivity of the nanoporous materials is extremely low due to its random structure. On the other hand, nanowires also have low thermal conductivities due to strong phonon scattering without any major decrease of electrical conductivity.[7] The operation of Si nanowires for thermoelectric applications is based on the large difference in the mean free path lengths of electrons and phonons at room temperature. Consequently, incorporating structures with critical dimensions/spacings smaller than the phonon mean free path should reduce the thermal conductivity without significantly affecting the electrical properties. Si nanowires are one type

of porous materials that keep electrical conduction paths because of their straight shape. Nanoporous should thus be a promising scalable thermoelectric nanostructured material with both good electrical properties and low thermal conductivity. We attempted to enhance *ZT* using nanoporous structures.[9,10] However, it was difficult to avoid a major reduction of the electrical conductivity, which was explained by the percolation theory.[11] A nanostructure containing isolated holes is necessary to decrease the thermal conductivity without significantly affecting the electrical conductivity, as already demonstrated for Si nanowires,[7] nanoporous Si,[12] and Al-doped ZnO containing nanovoids.[13]

Here, we present the fabrication process of a porous thin film of bismuth antimony telluride ($Bi_{0.4}Te_3Sb_{1.6}$). Porous alumina, as shown in Fig. 1, was generated in a two step anodizing process.[14] After preliminary washing of an Al plate, the surface oxide film was removed by electropolishing in a solution of perchloric acid and ethanol. The Al plate was anodized at a constant voltage of 20 V in sulfuric acid (0.3 wt. %) at 20 °C for 2 h. Then, the anodic oxide layer
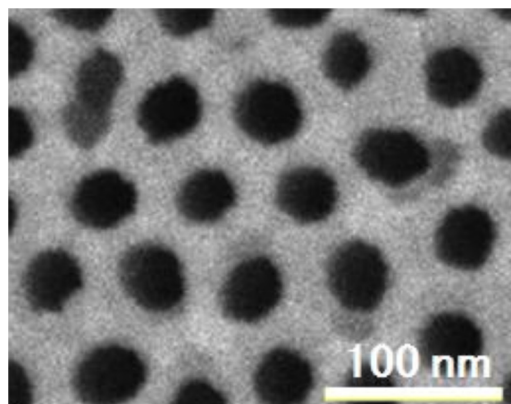

FIG. 1. (Color online) SEM image of alumina substrate containing 40 nm pores.

a)Electronic mail: j584102m@tobata.isc.kyutech.ac.jp.
b)Author to whom correspondence should be addressed. Electronic mail: miyazaki@mech.kyutech.ac.jp.
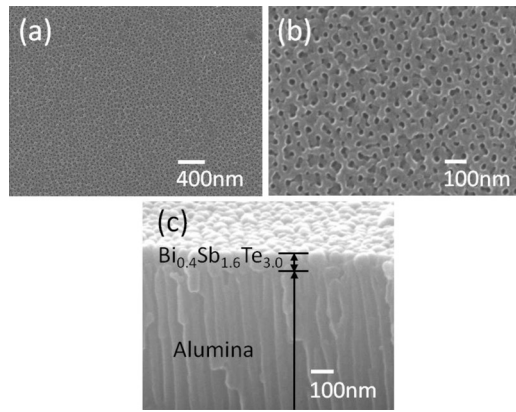c)Electronic mail: adachi@cstf.kyushu-u.ac.jp.

FIG. 2. SEM images of a porous thin film of bismuth antimony telluride. [(a) and (b)] Top view; (c) cross-sectional view.
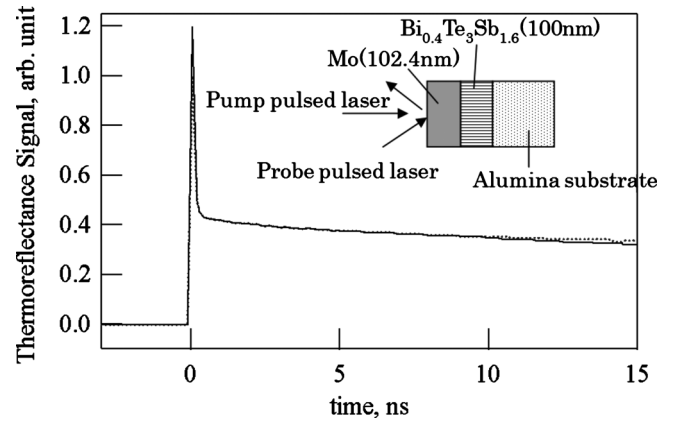

FIG. 3. Thermoreflectance signal as a function of delay time of the pump pulsed laser. The dashed and solid lines indicate experimental results and theoretical curve, respectively.

was removed by immersion in a solution of phosphoric acid (6 wt. %) and chromic acid (1.8 wt. %) at 60 °C for 14 h. After the removal of the anodic oxide layer, a pattern of pores was obtained on the surface of the Al substrate. The Al substrate was anodized again for 5 min at 20 V in sulfuric acid (0.3 wt. %) at 20 °C. Finally, the substrate was etched in a solution of phosphoric acid (5 wt. %) at 30 °C for 15 min.

A porous thermoelectric thin film was fabricated by depositing a thin film of $Bi_{0.4}Te_3Sb_{1.6}$ on the porous alumina substrate. Flash evaporation[15,16] was employed for depositing the thin film. Scanning electron microscope (SEM) images revealed that the thickness of the $Bi_{0.4}Te_3Sb_{1.6}$ film was 100 nm, while that of the porous alumina was 1 μm. The alumina substrate can be released after film deposition by chemical etching if required. SEM images of the fabricated porous $Bi_{0.4}Te_3Sb_{1.6}$ thin film are shown in Fig. 2. The average diameter of the holes was 20 nm and the average pitch of the hexagonally arranged holes was 50 nm. The packing density was 78%. If the holes are positioned randomly, the electrical conductivity decreased to one-fifth of that of the bulk value.[11]

The thermoelectric properties of the porous $Bi_{0.4}Te_3Sb_{1.6}$ thin film were measured at room temperature and are compared with parameters for typical $Bi_{0.4}Te_3Sb_{1.6}$ thin films in Table I. The in-plane electrical conductivity σ of the porous film was measured at room temperature by a four-point probe method with an accuracy of $\pm 3\%$. The measured value is proportional to the packing density of the material, which can be explained by the conventional model[18] related to the diffusive transport of electrons. The mean free path of electrons is considered to be shorter than the size of the pores in the fabricated film. The in-plane Seebeck coefficient S was also measured at room temperature with an accuracy of $\pm 5\%$. One end of the thin film is connected to a heat sink and the other end to a heater. The Seebeck coefficient is

determined as the ratio of the potential difference (ΔV) along the films to the temperature difference (ΔT). The thermal conductivity of the sample was 0.25 W/(m·K), which was measured by the picosecond thermoreflectance method with a fitting error of 0.05 W/(m·K) assuming the specific heat of bulk $Bi_{0.4}Te_3Sb_{1.6}$.[19–21] The measurement was carried out by a front-detection-front-heating as shown in Fig. 3. The molybdenum thin film was deposited on the top of the sample for light absorption layer. The penetration depth of a molybdenum thin film for wavelength of 780 nm is 18 nm.[20] Figure 3 shows the experimental result of temperature historical curve. At the zero in the delay time, both the pump and the probe pulsed lasers were simultaneously incident to the sample surface and the temperature on the front surface rose sharply. The heat propagates into the porous film and the substrate. The solid line in Fig. 3 indicates the surface temperature of Mo thin film $T_{Mo}(t)$ as a function of time as well as a theoretical curve calculated from the following equation:

$$T_{Mo}(t) = \frac{A}{\sqrt{t}}\left[1 + 2\sum_{n=1}^{\infty} \gamma^n \exp\left(-n^2\frac{\tau_{Mo}}{t}\right)\right]. \quad (2)$$

Here, the one-dimensional heat conduction is assumed. The influence of the alumina substrate does not appear in the measurement in nanoseconds by considering the thermal penetration depth. Here, γ is defined as

$$\gamma = \frac{b_{Mo} - b_{sample}}{b_{Mo} + b_{sample}}. \quad (3)$$

b is the thermal effusivity is given as

TABLE I. Thermoelectric properties of thin films of bismuth antimony telluride.

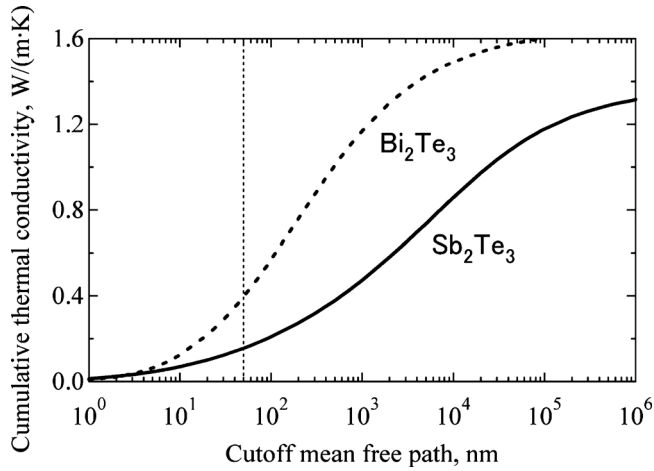|	σ (S/cm)	S (μV/K)	λ [W/(m·K)]	Reference
Flash evaporation $Bi_{0.4}Te_3Sb_{1.6}$	550	252	1.0	15
$Bi_{0.4}Te_3Sb_{1.6}$	610	160	⋯	17
Porous $Bi_{0.4}Te_3Sb_{1.6}$	398	198	0.25 ($\pm$0.05)	This work

FIG. 4. Cumulative thermal conductivities of Bi_2Te_3 and Sb_2Te_3 as a function of the cutoff mean free path of phonons.

$$b = \sqrt{\rho C \lambda}. \tag{4}$$

ρ, C, and λ are the density, specific heat capacity, and thermal conductivity. The τ_{Mo} in Eq. (2) is thermal diffusion time of Mo thin film.

$$\tau_{Mo} = \frac{d_{Mo}^2}{a_{Mo}}, \tag{5}$$

where d_{Mo} and a_{Mo} are the thickness and thermal diffusivity of Mo thin film. The C_{Mo} and ρ_{Mo} values were 249 J/(kg·K) and 10 220 kg/m^3.[20] The measured d_{Mo} was 102 nm. The values of C_{sample} and ρ_{sample} were 192 J/(kg·K) and 5265 kg/m^3. The ρ_{sample} is calculated from the bulk value 6750 kg/m^3 multiplied by the packing density 78%. The a_{Mo} and γ act as fitting parameters to match experimental results. When the γ is set to 1, b_{sample} must be 0. The physical meaning of this assumption is that the Mo thin film is thermally insulated. The a_{Mo} and γ were fitted to 1.4 $\times 10^{-5}$ m^2/s and 0.89 in the present study. Although the cross-plane thermal conductivity of the film was determined in the thermoreflectance measurements, the in-plane thermal conductivity is considered to be in the same order as that of the cross-plane. Cross-plane and in-plane thermal conductivities of nanostructured materials are usually both reduced by strong phonon scattering.[22,23] The measured thermal conductivity is in the same order as the theoretical minimum value[5,24,25] because long-range phonon transport is suppressed by the porous structure.

A model using a full distribution was employed to describe the phonon mean free path in the porous thin film.[26,27] The distribution function λ_L for the thermal conductivity per unit mean free path was calculated by using thermal conductivity of single crystals. The cumulative thermal conductivity $\lambda(l)$ caused by phonons with a mean free path between 0 and l

$$\lambda(l) = \int_0^l \lambda_L dL, \tag{6}$$

where l, the cutoff mean free path, was plotted. The cumulative thermal conductivities of Bi_2Te_3 and Sb_2Te_3 as a function of the mean free path are depicted in Fig. 4. It is considered that the curve calculated for the Sb_2Te_3 can be applied to the $Bi_{0.4}Te_3Sb_{1.6}$ because the structures of both

compounds are similar. When the cutoff mean free path is greater than 100 μm, the cumulative thermal conductivity of the Sb_2Te_3 reaches approximately that of a single crystal. The cumulative thermal conductivity is reduced as the cutoff mean free path decreases. The experimental result [0.25 W/(m·K) with electronic thermal conductivity] is fairly similar to the calculated value [0.155 W/(m·K)] for the model at a cutoff mean free path of 50 nm. Here, the cutoff mean free path was estimated according to the average pore spacing. The significant reduction of the thermal conductivity is caused by significant scattering of long-range phonons by the pores in the thin film.

In summary, the figure of merit of $Bi_{0.4}Te_3Sb_{1.6}$ was enhanced to 1.8 at room temperature (300 K) by the formation of a porous thin film, although the measurement error was 13% for the power factor and 28% for ZT by propagation of uncertainty from the σ, S, and λ measurements. The thermal conductivity was reduced without any major decrease in the electrical conductivity because of the hexagonal arrangement of the pores. The reduced thermal conductivity was consistent with a value calculated using a model for the full distribution of phonon mean free paths.

[1] G. J. Snyder and E. S. Toberer, Nature Mater. **7**, 105 (2008).
[2] L. D. Hicks and M. S. Dresselhaus, Phys. Rev. B **47**, 12727 (1993).
[3] D. G. Cahill, W. K. Ford, K. E. Goodson, G. D. Mahan, A. Majumdar, H. J. Maris, R. Merlin, and S. R. Phillpot, J. Appl. Phys. **93**, 793 (2003).
[4] G. Chen and A. Shakouli, J. Heat Transfer **124**, 242 (2002).
[5] R. Venkatasubramanian, E. Siivola, T. Colpitts, and B. O'Quinn, Nature (London) **413**, 597 (2001).
[6] T. C. Harman, P. J. Taylor, M. P. Walsh, and B. E. LaForge, Science **297**, 2229 (2002).
[7] A. I. Hochbaum, R. Chen, R. D. Delgado, W. Liang, E. C. Garnett, M. Najarian, A. Majumdar, and P. Yang, Nature (London) **451**, 163 (2008).
[8] D. W. Song, W.-N. Shen, B. Dunn, C. D. Moore, M. S. Goorsky, T. Radetic, R. Gronsky, and G. Chen, Appl. Phys. Lett. **84**, 1883 (2004).
[9] M. Takashiri, S. Tanaka, M. Takiishi, M. Kihara, K. Miyazaki, and H. Tsukamoto, J. Alloys Compd. **462**, 351 (2008).
[10] K. Miyazaki, Proceedings of ASME Second Micro/Nano Heat and Mass Transfer International Conference, MNHT2009-18247, 2009.
[11] B. J. Last and D. J. Thouless, Phys. Rev. Lett. **27**, 1719 (1971).
[12] A. Yamamoto, M. Takimoto, T. Ohta, K. Sakamoto, K. Miki, L. Whitlow, K. Kamisako, and T. Matsui, Proceedings of 17th International Conference on Thermoelectrics, 1998, p. 198.
[13] M. Ohtaki, R. Hayashi, and K. Araki, Proceedings of 26th International Conference on Thermoelectrics, 2007, p. 112.
[14] H. Masuda and M. Satoh, Jpn. J. Appl. Phys., Part 2 **35**, L126 (1996).
[15] M. Takashiri, K. Miyazaki, and H. Tsukamoto, Thin Solid Films **516**, 6336 (2008).
[16] M. Takashiri, T. Shirakawa, K. Miyazaki, and H. Tsukamoto, J. Alloys Compd. **441**, 246 (2007).
[17] I. H. Kim, Mater. Lett. **44**, 75 (2000).
[18] Z. Hashin and S. Shtrikman, J. Appl. Phys. **33**, 3125 (1962).
[19] N. Taketoshi, T. Baba, and A. Ono, Rev. Sci. Instrum. **76**, 094903 (2005).
[20] N. Taketoshi, T. Baba, E. Schaub, and A. Ono, Rev. Sci. Instrum. **74**, 5226 (2003).
[21] K. Kuwahara, O. Suzuki, S. Takada, N. Hata, P. Fons, and J. Tominaga, Microelectron. Eng. **86**, 1009 (2009).
[22] W. K. Liebmann and E. A. Miller, J. Appl. Phys. **34**, 2653 (1963).
[23] G. Chen, C. L. Tien, X. Wu, and J. S. Smith, J. Heat Transfer **116**, 325 (1994).
[24] D. G. Cahill, S. K. Watson, and R. O. Pohl, Phys. Rev. B **46**, 6131 (1992).
[25] B.-L. Huang and M. Kaviany, Phys. Rev. B **77**, 125209 (2008).
[26] J. Callaway, Phys. Rev. **113**, 1046 (1959).
[27] C. Dames and G. Chen, J. Appl. Phys. **95**, 682 (2004).